ACCOUNTS of chemical research

Article

pubs.acs.org/accounts

Gas Phase Studies of the Pesci Decarboxylation Reaction: Synthesis, Structure, and Unimolecular and Bimolecular Reactivity of Organometallic Ions

Richard A. J. O'Hair*[,†,‡,§] and Nicole J. Rijs[†,‡,§,∥]

[†]School of Chemistry, University of Melbourne, Melbourne, Victoria 3010, Australia

[‡]Bio21 Institute of Molecular Science and Biotechnology, The University of Melbourne, Melbourne, Victoria 3010, Australia

[§]ARC Centre of Excellence in Free Radical Chemistry and Biotechnology, The University of Melbourne, Melbourne, Victoria 3010, Australia

[∥]Institut für Chemie, Technische Universität Berlin, Straße des 17. Juni 115, 10623 Berlin, Germany

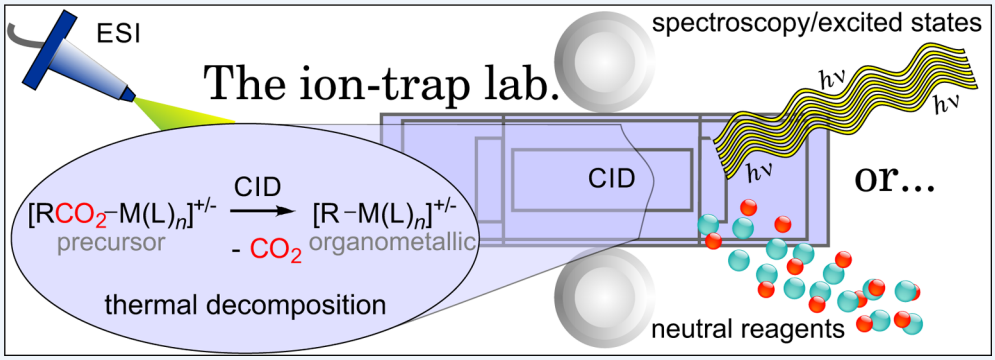

CONSPECTUS: Decarboxylation chemistry has a rich history, and in more recent times, it has been recruited in the quest to develop cheaper, cleaner, and more efficient bond-coupling reactions. Thus, over the past two decades, there has been intense investigation into new metal-catalyzed reactions of carboxylic substrates. Understanding the elementary steps of metal-mediated transformations is at the heart of inventing new reactions and improving the performance of existing ones. Fortunately, during the same time period, there has been a convergence in mass spectrometry (MS) techniques, which allows these catalytic processes to be examined efficiently in the gas phase. Thus, electrospray ionization (ESI) sources have been combined with ion-trap mass spectrometers, which in turn have been modified to either accept radiation from tunable OPO lasers for spectroscopy based structural assignment of ions or to allow the study of ion–molecule reactions (IMR). The resultant "complete" gas-phase chemical laboratories provide a platform to study the elementary steps of metal-catalyzed decarboxylation reactions in exquisite detail.

In this Account, we illustrate how the powerful combination of ion trap mass spectrometry experiments and DFT calculations can be systematically used to examine the formation of organometallic ions and their chemical transformations. Specifically, ESI-MS allows the transfer of inorganic carboxylate complexes, $[RCO_2M(L)_n]^x$, (x = charge) from the condensed to the gas phase. These mass selected ions serve as precursors to organometallic ions $[RM(L)_n]^x$ via neutral extrusion of CO_2, accessible by slow heating in the ion trap using collision induced dissociation (CID). This approach provides access to an array of organometallic ions with well-defined stoichiometry. In terms of understanding the decarboxylation process, we highlight the role of the metal center (M), the organic group (R), and the auxiliary ligand (L), along with cluster nuclearity, in promoting the formation of the organometallic ion. Where isomeric organometallic ions are generated and normal MS approaches cannot distinguish them, we describe approaches to elucidate the decarboxylation mechanism via determination of their structure. These "unmasked" organometallic ions, $[RM(L)_n]^x$, can also be structurally interrogated spectroscopically or via CID. We have thus compared the gas-phase structures and decomposition of several highly reactive and synthetically important organometallic ions for the first time. Perhaps the most significant aspect of this work is the study of bimolecular reactions, which provides experimental information on mechanistically obscure bond-formation and cross-coupling steps and the intrinsic reactivity of ions. We have sought to understand transformations of substrates including acid–base and hydrolysis reactions, along with reactions resulting in C–C bond formation. Our studies also allow a direct comparison of the performance of different metal catalysts in the individual elementary steps associated with protodecarboxylation and decarboxylative alkylation cycles. Electronic structure (DFT and ab initio) and dynamics (RRKM) calculations provide further mechanistic insights into these reactions.

The broad implications of this research are that new reactions can be discovered and that the performance of metal catalysts can be evaluated in terms of each of their elementary steps. This has been particularly useful for the study of metal-mediated decarboxylation reactions.

Received: October 12, 2014
Published: January 16, 2015

DOI: 10.1021/ar500377u
Acc. Chem. Res. 2015, 48, 329–340

1. INTRODUCTION

Carboxylic acids are desirable substrates, because they are readily available, are easy to handle, exhibit structural diversity, and are "green" alternatives to existing reagents.[1] They are used in many traditional "textbook" reactions (Scheme 1a, X = OH)[2] and in synthetically valuable decarboxylative bond-transformation protocols (eqs 11−18, Scheme 1b,c).

In the absence of a metal-catalyst, high temperatures are required for decarboxylation, and side-products are often formed. For example, pyrolysis of acetic acid requires temperatures >500 °C, with decarboxylation (eq 19) proceeding half as much as dehydration (eq 20).[2]

$$MeCO_2H \rightarrow CH_4 + CO_2 \quad (19)$$

$$MeCO_2H \rightarrow CH_2CO + H_2O \quad (20)$$

Organometallics can be synthesized via decarboxylation (eq 21, where M = metal, L_n = coordinating ligand(s), and x = charge).[3] The reverse reaction is used to synthesize carboxylic acids (eq 22).[4] Metal-catalyzed decarboxylation does not always proceed via the formation of an organometallic intermediate. Reactions occurring via Lewis acid catalysis[5] (including enzyme reactions[6] and the formation of enolates[7]), photochemically, electrolytically or via carboxylate radicals (eq 23) or anions (eq 24) are not considered here.

$$[RCO_2M(L)_n]^x \rightarrow [RM(L)_n]^x + CO_2 \quad (21)$$

$$[RM(L)_n]^x + CO_2 \rightarrow [RCO_2M(L)_n]^x \quad (22)$$

$$RCO_2^{\bullet} \rightarrow R^{\bullet} + CO_2 \quad (23)$$

$$RCO_2^{-} \rightarrow R^{-} + CO_2 \quad (24)$$

The "Pesci" reaction has an interesting history. Leone Pesci's seminal work on the decarboxylative formation of organomercury upon heating of phthalic acid (Figure 1b,c)[8] was followed by Whitmore's discovery that CO_2H could be replaced by either H or Br (Figure 1c).[9] Kharasch wanted to exploit these organomercury compounds for C−X and C−C bond-formation (Figure 1d).[10]

Shepard, Winslow, and Johnson pioneered copper-catalyzed protodecarboxylation reactions of halogenated furoic acid derivatives,[11] a reaction subsequently developed into an analytical protocol.[12] Evidence for the formation of organocopper intermediates had to wait until Nilsson's series of landmark papers, where they were intercepted by reactive electrophiles.[13]

Transient organometallic species are implicated in many decarboxylative-coupling reactions.[14] Groundbreaking studies on palladium-catalyzed decarboxylative-coupling reactions by Myers,[15] Gooßen,[16] and others, and mechanistic studies by Liu[17] have highlighted several modes of reactivity (Scheme 1b). The decarboxylative coupling of R^1 and R^2 groups of single carboxylic esters, $R^1CO_2R^2$ (Scheme 1c, Figure 1d), has also been realized.[18] The key to effective use of decarboxylative-coupling reactions is an understanding of the underlying reaction mechanisms, which has been the motivation for our gas-phase studies.

2. DECARBOXYLATION IN THE GAS PHASE

Collision-induced dissociation (CID) has been used to examine the gas phase formation of "bare" carbanions from carboxylate anions (eq 24).[19] Early studies of metal carboxylates were limited by the available ionization methods, which required vaporizable metal carboxylates[20] and few of these studies used tandem mass spectrometry (MS) to probe decarboxylation.[21]

Electrospray ionization (ESI) transfers inorganic and organometallic ions to the gas phase,[22] where the multistage mass spectrometry (MS^n) capabilities of ion-trap mass spectrometers can be used to study their structure and reactivity.[23] These "complete chemical laboratories" (Figure 2) provide a platform to probe mechanistic details for the formation of organometallic ions and their subsequent reactions when subjected to heat (under CID)[23d] or light or with neutral reagents (essentially proceeding at room temperature[24]).

Scheme 1. Carboxylic Acid Substrates: (a) "Textbook" Reactions, (b) Metal-Catalyzed Decarboxylation To Form an Organometallic Intermediate, Which Undergoes Subsequent C−X Bond Formation, and (c) Metal-Catalyzed Oxidative Insertion of Esters with Subsequent Decarboxylation and C−C Bond Coupling

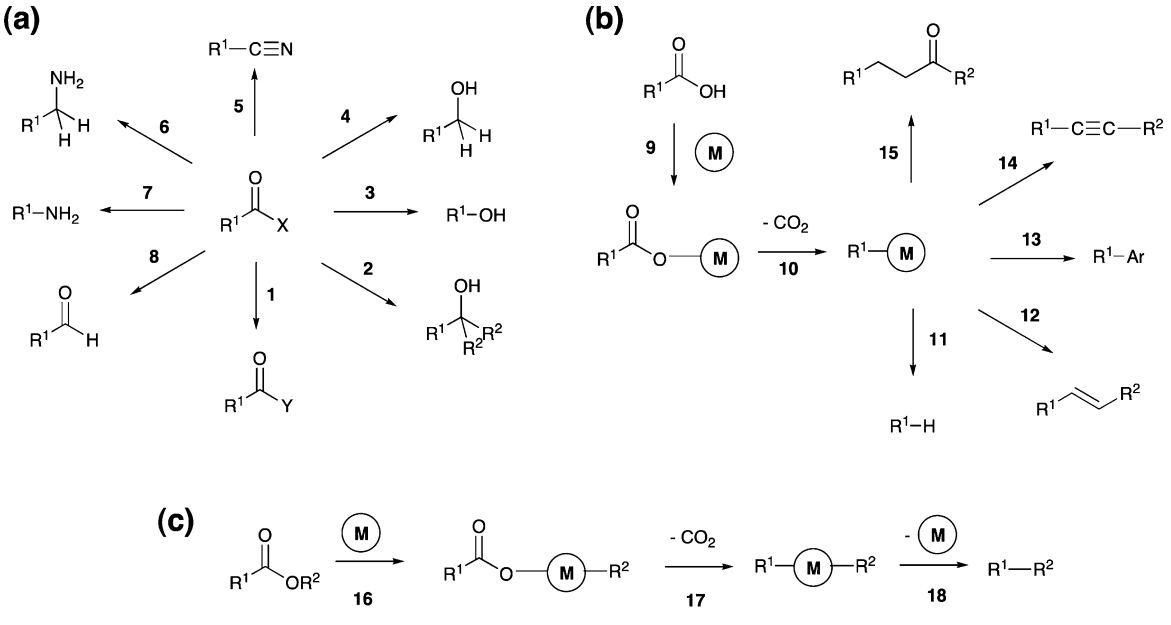

DOI: 10.1021/ar500377u
Acc. Chem. Res. 2015, 48, 329−340

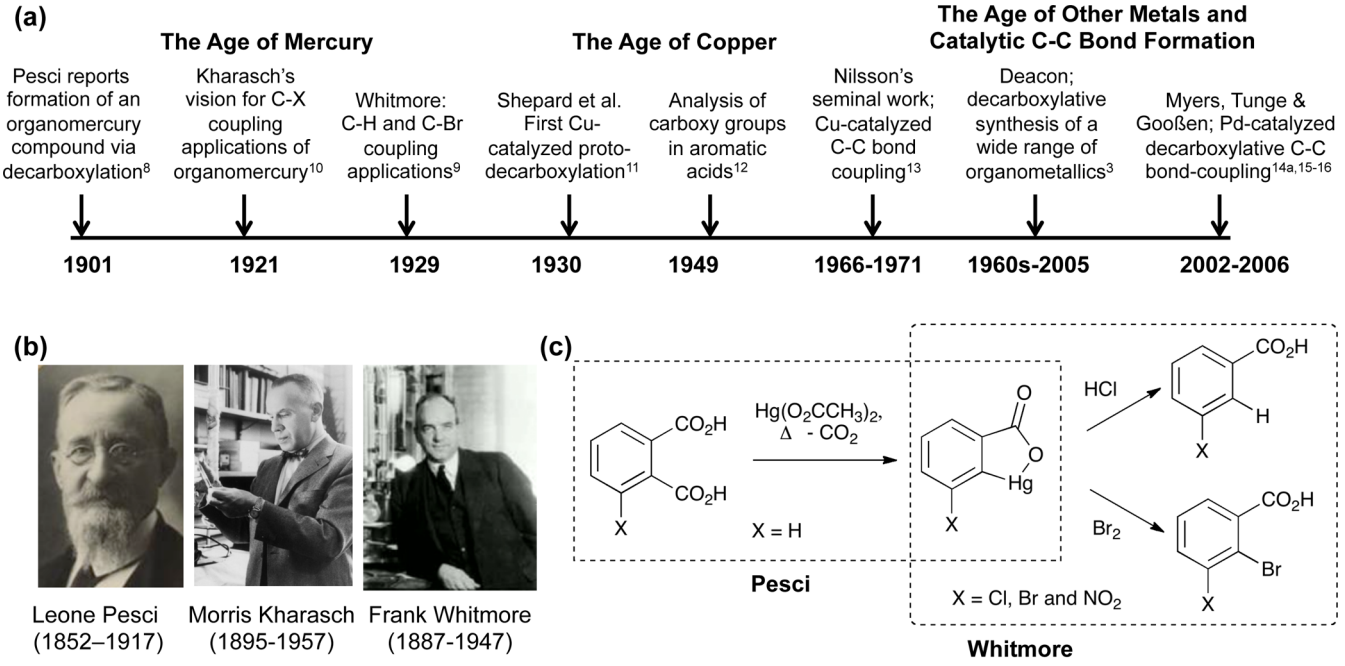

"The above mentioned method for the preparation of mercury compounds by heating the mercury salt of an acid, which loses carbon dioxide readily, would thereby enable us to replace a carboxyl group by a halogen and it is also hoped that it would have a much wider application in that by heating the mercury compound, thus formed, in the dry state or in some solvent the mercury would oxidize one of the carbons and thereby link the two carbons together." Kharasch[10]

Figure 1. (a) Timeline of the Pesci decarboxylation reaction, (b) the "founding fathers" (adapted with permission from photographs in the Archives at the Universities of Bologna, Chicago (Photographic Archive, apf1-03214, Special Collections Research Center), University of Chicago Library, and Penn State University (Frank Whitmore papers, 1928−1951, PSUA 725, Penn State University Archives, Special Collections Library, University Libraries, Pennsylvania State University)), (c) Pesci's report (X = H) and Whitmore's subsequent coupling reactions, and (d) Kharasch's vision.

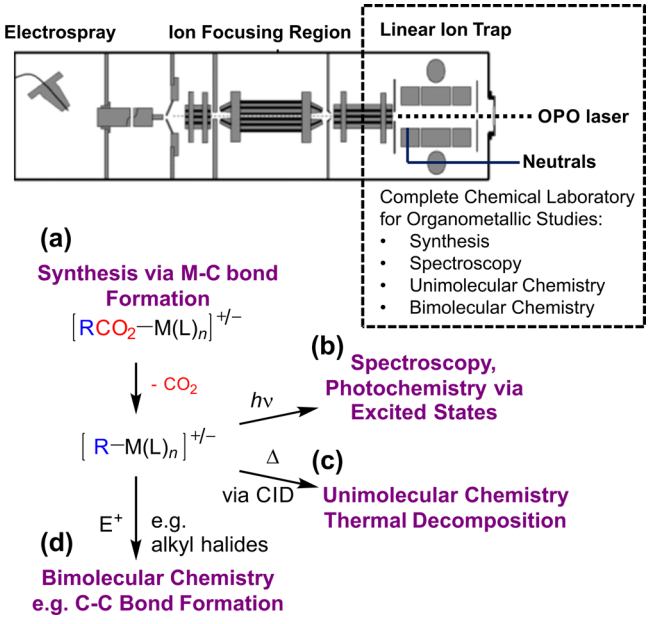

Figure 2. MS^n experiments allow examination of organometallic (a) formation via decarboxylation, (b) spectra (for UV−vis spectra, this provides information on photochemical fragmentation via excited states), (c) CID, and (d) bimolecular reactivity.

A key requirement for our studies is that precursor and product must have a net positive or negative charge (Scheme 2). Cations can be formed from neutral carboxylates via loss of a carboxylate anion[25] or via addition of a metal cation (Scheme 2a,b).[26] Anions can be formed from neutral carboxylates via addition of a carboxylate anion,[27] deprotonation of a second carboxylate site,[28] or addition of a fixed charge ligand (Scheme 2c−e, respectively).[29]

3. ENERGETIC REQUIREMENTS FOR DECARBOXYLATION

Decarboxylative organometallic formation requires rearrangement (Figure 3) via a tight transition state (TS). While geometrically distinct, all of these TSs involve breaking of C−C and M−O bonds and formation of a M−C bond.

Decarboxylation must be among the lowest energy pathways available (Figure 4). Anionic metal carboxylates $[RCO_2M(L)_n]^-$ have three potential decomposition pathways: decarboxylation (eq 25), elimination of carboxylate anion (eq 26), or elimination of auxiliary ligand (eq 27). To be competitive, the decarboxylation activation energy (eq 25, E_{act}) should be below the heterolytic bond energies (D) of both the carboxylate (eq 26, $D(M-O^-)$) and auxiliary ligand (eq 27, $D(M-L^-)$). This competition (Table 1) is influenced by the R group, metal center, cluster nuclearity, and auxiliary ligand.

$$[RCO_2M(L)_n]^- \rightarrow [RM(L)_n]^- + CO_2 \quad (25)$$

$$[RCO_2M(L)_n]^- \rightarrow RCO_2^- + [M(L)_n] \quad (26)$$

$$[RCO_2M(L)_n]^- \rightarrow [RCO_2M(L)_{n-1}] + L^- \quad (27)$$

DOI: 10.1021/ar500377u
Acc. Chem. Res. 2015, 48, 329−340

Scheme 2. Generating Desired Precursor and Organometallic Product with a Net Positive or Negative Charge

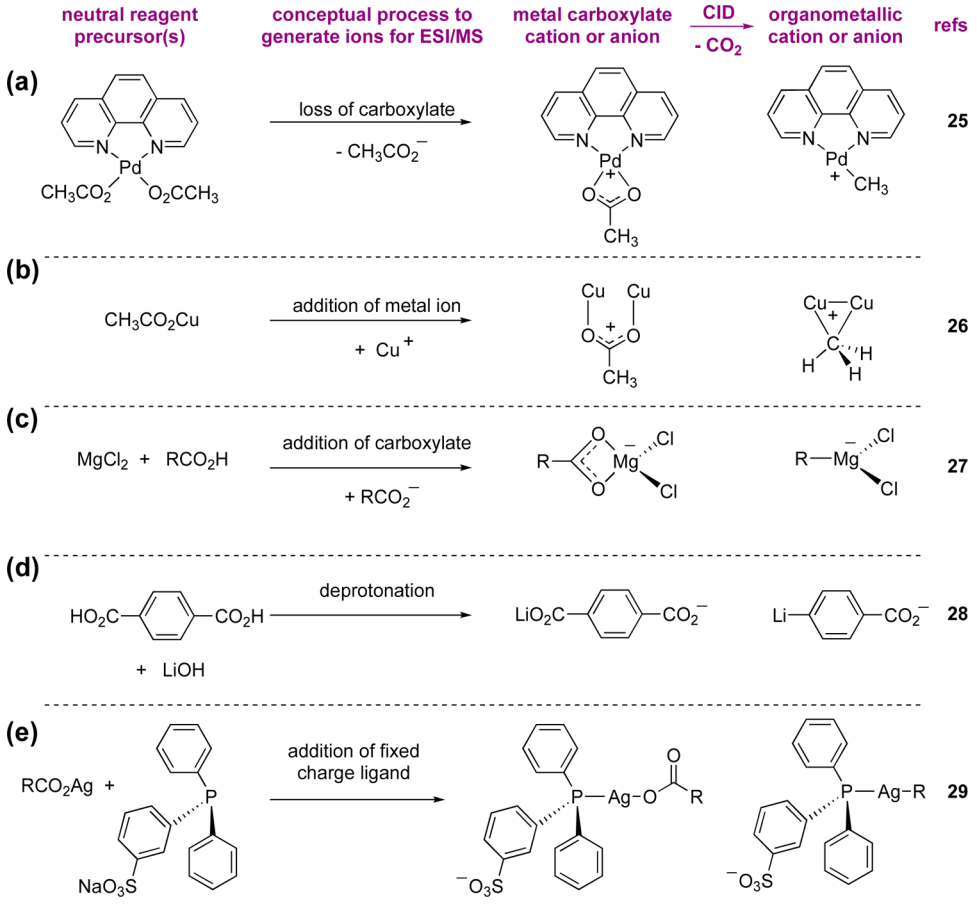

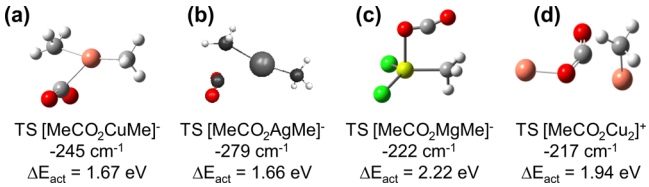

Figure 3. TS geometries and imaginary frequencies for decarboxylation. Energies are relative to parent species (DFT methods detailed in refs 27e, f, b, and 26a for a–d, respectively).

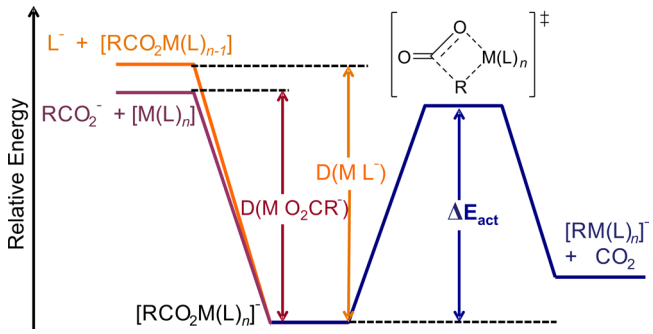

Figure 4. Simplified potential energy diagram for the decomposition of anionic metal carboxylates, $[RCO_2M(L)_n]^-$ showing the competition between decarboxylation (eq 25) and barrierless elimination of the carboxylate (eq 26) or ligand (eq 27) anions, respectively.

3.1. R Group

The R group can promote or limit decarboxylation via its bulkiness, flexibility, and hybridization. For example, though chloride elimination (eq 27) directly competes with decarboxylation (eq 25) of the magnesium carboxylates, $[RCO_2Mg(Cl)_2]^-$ (Table 1, R = alkyl, entries 1 and 5–8),[27b,q] unsaturated and unhindered R substituents promote decarboxylation and minimize chloride loss (Table 1, entries 9–14).[27g,q] Likewise for copper and silver carboxylates (Figure 5), decarboxylation is competitive for R = Me, but carboxylate loss outcompetes when R is sterically hindered (R = *i*Pr and *t*Bu), and the energetic requirement is lowered with unsaturated ligands (R = allyl, $PhCH_2$, and Ph), due to the favorable distribution of electron density in the decarboxylation TS.[27e,f] The relative ease of decarboxylation for each R has been determined via CID of mixed dicarboxylates, $[R^1CO_2MO_2CR^2]^-$ (M = Cu or Ag). Reaction of the isomeric organocuprates $[MeCuO_2CR]^-$ and $[MeCO_2CuR]^-$ with allyl iodide reports on the site(s) of decarboxylation (eq 28 versus 29).[27e] Regiospecifically ^{13}C labeled silver carboxylates, $[Me^{13}CO_2AgO_2CR]^-$, reveal the selectivity directly via $^{13}CO_2$ (eq 30) versus CO_2 (eq 31) extrusion,[27f] as illustrated for R = Ph (Figure 6). The decarboxylation regioselectivity of $[(MeCO_2)Pd(CH_2CO_2)]^-$ was also determined using these methods.[27p]

$$[MeCuO_2CR]^- + C_3H_5I \rightarrow [ICuO_2CR]^- + C_3H_5Me \quad (28)$$

$$[MeCO_2CuR]^- + C_3H_5I \rightarrow [MeCO_2CuI]^- + C_3H_5R \quad (29)$$

DOI: 10.1021/ar500377u
Acc. Chem. Res. 2015, 48, 329–340

Table 1. Experimentally Observed $[RCO_2Mg(L)_n]^-$ Decomposition and Predicted Relative Energetics[a]

		decarb (eq 25)		L^- elim (eq 27)		RCO_2^- elim (eq 26)	
		obsd?	ΔE[b]	obsd?	ΔE[c]	obsd?	ΔE[c]
$[MeCO_2Mg(L)_2]^-$	L =						
1	Cl[d]	+++	2.22	+++	2.40	x	3.42
2	Br[e]	++	2.22	+++	2.12	x	3.42
3	I[e]	x	2.22	+++	1.81	x	3.44
4	$MeCO_2$[d]	+++	2.35	+++	2.24	+++	2.24
$[RCO_2Mg(Cl)_2]^-$	R =						
5	Et[e]	++	2.42	+++	2.40	x	3.40
6	Pr[e]	++	2.44	+++	2.41	x	3.38
7	*i*Pr[e]	++	2.53	+++	2.40	x	3.37
8	*t*Bu[e]	+	2.64	+++	2.41	x	3.35
9	vinyl[e]	+++	2.20	++	2.40	x	3.31
10	allyl[e]	+++	2.05	++	2.46	x	3.26
11	HC≡C[f]	+++	1.33	+	2.57	x	3.03
12	Ph[e]	+++	2.27	++	2.42	x	3.22
13	$PhCH_2$[e]	+++	2.08	+	2.44	x	3.19
14	$PhCH_2CH_2$[e]	+++	2.32	+++	2.46	x	3.29

[a] ΔE, in eV, eqs 25−27 and Figure 3. Relative yields +++ = major, ++ = minor, + = very minor, x = not observed. [b] Activation energy. [c] Separated products, assumed barrierless (Figure 4). [d] Reference 27b. [e] Reference 27q. [f] Reference 27g.

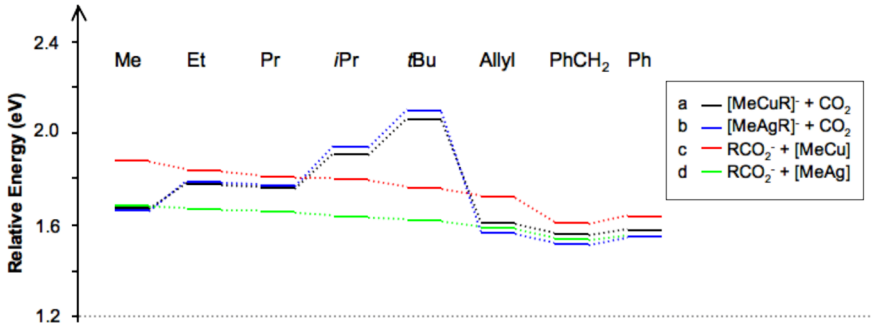

Figure 5. Comparison of the decarboxylation activation energy versus the energetics of carboxylate loss from $[RCO_2M(Me)]^-$, where M = Ag and Cu and R = Me, Et, Pr, *i*Pr, *t*Bu, Allyl, $PhCH_2$, and Ph.

$$[Me^{13}CO_2AgO_2CR]^- \rightarrow [MeAgO_2CR]^- + {}^{13}CO_2 \quad (30)$$

$$[Me^{13}CO_2AgO_2CR]^- \rightarrow [Me^{13}CO_2AgR]^- + CO_2 \quad (31)$$

3.2. Metal Center

Decarboxylation at a metal center is controlled by the starting geometry of the complex (e.g., mono- or bidentate) and metal-based orbitals, which facilitate the rearrangement process. Changing the metal center can therefore alter the competiveness of decarboxylation. For example, decarboxylation of alkali earth acetate anions competes with ligand loss (Figure 7b,d). In contrast, the dominant pathway for alkaline earth acetate anions is ligand loss (Figure 7a,c).[27d]

Decarboxylation readily occurs at copper,[27c,e] consistent with the widespread use of copper catalysts in the condensed phase. The success of copper can be largely attributed to its nucleophilicity. Although the activation barriers for decarboxylation at silver are very similar to those of copper (Figure 5), the weaker Ag−L bonds allow silver carboxylates to eliminate the carboxylate ligand (eq 26).[27a,f] On the other hand, gold has stronger Au−L bonds, and decarboxylation is efficient.[27j] For coinage metal carboxylates possessing a fixed charge phosphine ligand (Scheme 2e), similar trends were observed: copper complexes undergo decarboxylation in competition with phosphine ligand loss; silver complexes are prone to phosphine ligand loss. With the exception of R = Ph, gold complexes undergo more ligand loss in this case, because they have a higher barrier to decarboxylation (Figure 8).[29]

The decarboxylation TS geometries of coinage metal carboxylates $[CX_3CO_2M(CX_3)]^-$ (X = H or F) are similar (Figure 9), the linearity distorted by 12−15° in each case, though M = Au possesses a late TS, with a shorter C−C bond in the bond-breaking carboxylate moiety and a smaller angle. As a consequence of differences in bonding and nucleophilicity, the activation energy for decarboxylation when M = Cu and Au significantly increases with the electron withdrawing CF_3 group (Figure 9).[27l] In contrast, there is little variation in the decarboxylation TS energy for silver complexes, making sequential decarboxylation a viable route to synthesize both $[MeAgMe]^-$ and $[CF_3AgCF_3]^-$.

3.3. Nuclearity of the Metal

A second metal center can work in synergy to promote decarboxylation reactions. For example, comparison of mononuclear and binuclear magnesium carboxylates (Figure 10) reveals that $[HCCO_2Mg_2(Cl)_4]^-$ is able to undergo a six-centered TS in which both metal centers play a role in decarboxylation (eq 32), which also results in the thermodynamically favored bridged acetylide.[27g]

$$[RCO_2M_y(L)_n]^- \rightarrow [RM_y(L)_n]^- + CO_2 \quad (32)$$

However, the additional metal center may also open additional low energy decompositions. For example, other reactions

DOI: 10.1021/ar500377u
Acc. Chem. Res. 2015, 48, 329−340

competing with decarboxylation of the coinage metal acetate cations (Scheme 2b) include CO elimination for $[MeCO_2Cu_2]^+$ and $Me^\bullet$ for $[MeCO_2CuAg]^+$.[26a]

3.4. Auxiliary Ligand

To facilitate decarboxylation, the auxiliary ligand must (1) be strongly bound to the metal, to not be eliminated under CID conditions, (2) not decompose itself, (3) have a denticity that allows for interaction of the CO_2 moiety with the metal center in the decarboxylation TS, and (4) provide the necessary orbital contribution to modulate the metal center in the decarboxylation TS.

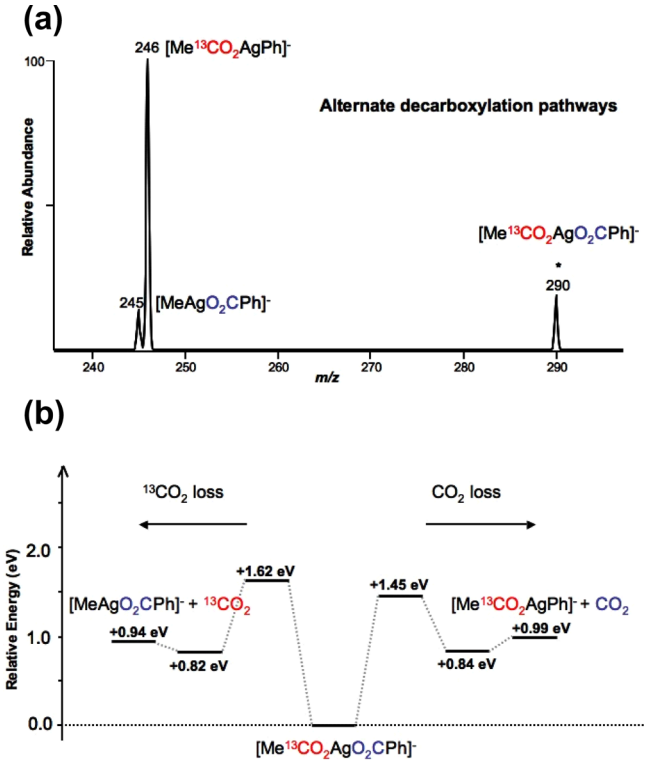

Figure 6. (a) Decarboxylation of mass-selected (*) $[Me^{13}CO_2AgO_2CPh]^-$ provides direct evidence for the site of decarboxylation via $^{13}CO_2$ (eq 30) versus CO_2 loss (eq 31); (b) DFT calculated energy surface for these competing losses.

While the decarboxylation barrier of $[MeCO_2Mg(L)_2]^-$ (L = Cl, Br and I) is unaffected by the change in L (as might be expected for an ionic interaction between Mg and L), the stability of L dictates whether decarboxylation will compete with ligand loss.[27b,q] For example, decarboxylation occurs when L = Cl but not when L = I (Table 1, entries 1 and 3). Thus, Br and I are poor auxiliary ligands.

Auxiliary ligand decomposition is highly ligand dependent. When we compare sulfinate (L = $MeSO_2$) versus sulfonate (L = $MeSO_3$) ligands in $[MeCO_2Cu(L)]^-$ complexes, for L = $MeSO_2$ (Figure 11a), desulfination (eq 33) is preferred over decarboxylation (eq 34).[27m] In contrast, for L = $MeSO_3$ (Figure 11b), desulfonation (eq 35) is disfavored compared with decarboxylation (eq 36). Thus, sulfonate is a superior auxiliary ligand.

$$[MeCO_2CuO_2SMe]^- \rightarrow [MeCO_2CuMe]^- + SO_2 \quad (33)$$

$$[MeCO_2CuO_2SMe]^- \rightarrow [MeCuO_2SMe]^- + CO_2 \quad (34)$$

$$[MeCO_2CuO_3SMe]^- \rightarrow [MeCO_2CuMe]^- + SO_3 \quad (35)$$

$$[MeCO_2CuO_3SMe]^- \rightarrow [MeCuO_3SMe]^- + CO_2 \quad (36)$$

Trifluoroacetate ligands also suffer ligand decomposition, with concurrent loss of CF_2 (eq 37) depleting the desired M−C bond formation.[27l] Efforts to carry out decarboxylative trifluoromethylations with copper are inherently limited by this competitive process.

$$[CF_3CO_2Cu(L)]^- \rightarrow [FCu(L)]^- + CO_2 + CF_2 \quad (37)$$

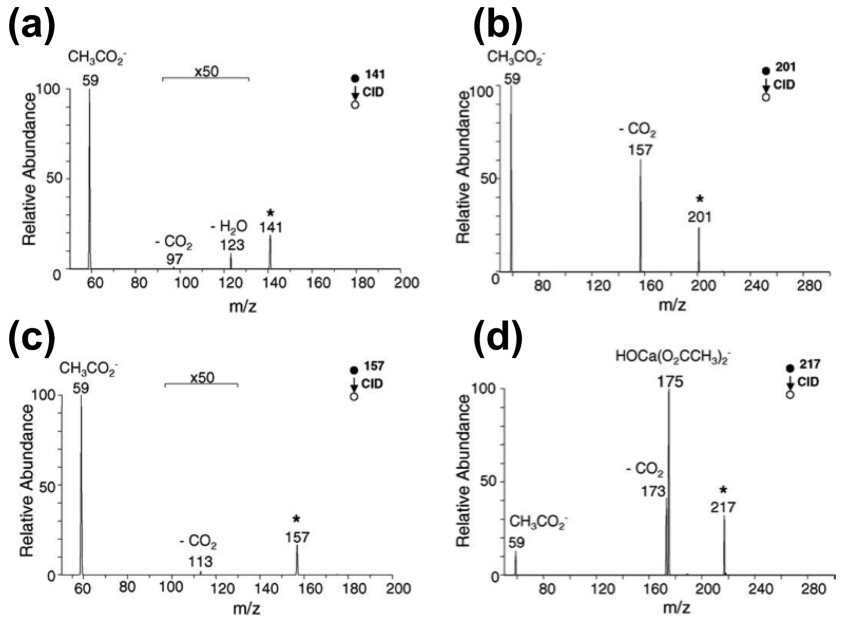

Figure 7. CID spectra of mass-selected (*) (a) $[MeCO_2Na(O_2CMe)]^-$, (b) $[MeCO_2Mg(O_2CMe)_2]^-$, (c) $[MeCO_2K(O_2CMe)]^-$, and (d) $[MeCO_2Ca(O_2CMe)_2]^-$.

DOI: 10.1021/ar500377u
Acc. Chem. Res. 2015, 48, 329−340

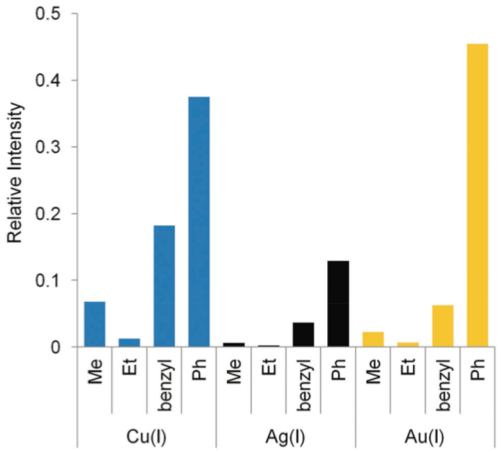

Figure 8. Comparison of decarboxylation ability for the complexes $[RCO_2M(TPPMS)(I)]^-$ (M = Cu, Ag, Au; R = Me, Et, Ph, benzyl). Relative intensity on the *y*-axis is the ratio of the signal intensity of decarboxylated product ion divided by reactant ion.

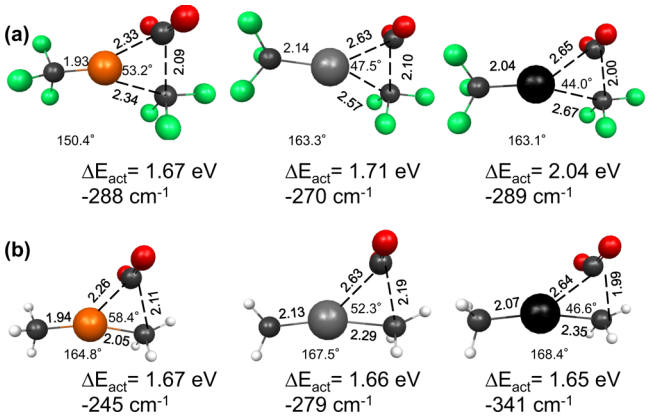

Figure 9. Comparison of TS geometries and vibrational frequencies for decarboxylation of (a) $[CF_3CO_2M(CF_3)]^-$ and (b) $[MeCO_2M(Me)]^-$, M = Cu, Ag, and Au. Angles refer to C−M−C angles.

4. UNIMOLECULAR REACTIONS OF ORGANOMETALLIC IONS

4.1. Low Energy CID

The slow heating of organometallic ions by low energy CID reveals decomposition pathways.[23d] These include homolysis (eqs 38 and 39), heterolysis (eq 40), *β*-hydride elimination (eq 41), and reductive elimination (eq 42). The competitiveness of each pathway is metal-dependent. For example, (i) as a consequence of differences in M−C bond strengths, organocuprates undergo *β*-hydride elimination, while organoargenates prefer Ag−C bond-homolysis;[27i] (ii) as a consequence of differences in preferred oxidation states (reduction to Pd(0) versus Ni(II)), $[PdC_2H_5]^-$ prefers *β*-hydride elimination, while $[NiC_2H_5]^-$ does not.[27p] Dinuclear species are more efficient at promoting both decarboxylation and coupling in the Glaser-like decarboxylative C−C bond-coupling of alkynyl carboxylic acids (eq 42) mediated by cobalt chloride anions ($[Co_xCl_y(R)_2]^-$, eq 43).[27s]

$$[MeMR]^- \rightarrow [RM]^{-\bullet} + Me^{\bullet} \quad (38)$$

$$[MeMR]^- \rightarrow [MeM]^{-\bullet} + R^{\bullet} \quad (39)$$

$$[MeMR]^- \rightarrow R^- + [MeM] \quad (40)$$

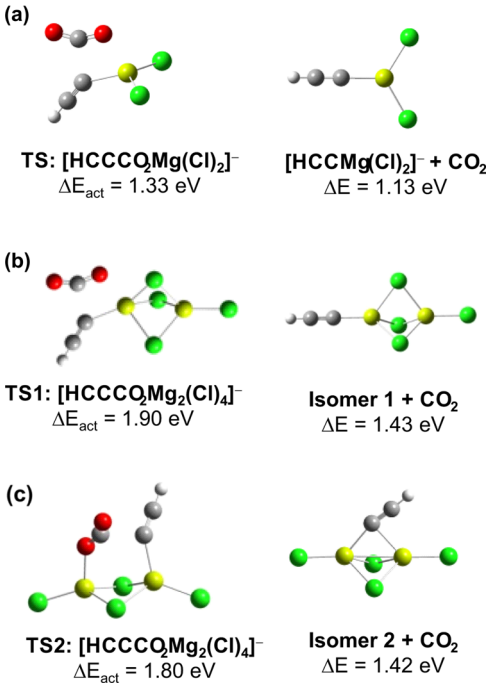

Figure 10. TS geometries and products associated with the decarboxylation of (a) $[HCCCO_2Mg(Cl)_2]^-$ (eq 25) or $[HCCCO_2Mg_2(Cl)_4]^-$ isomers to yield isomeric $[HCCMg_2(Cl)_4]^-$ (eq 32) with (b) terminal acetylide or (c) bridged acetylide.

$$[MeMR]^- \rightarrow [MeMH]^- + [R{-}H] \quad (41)$$

$$2RC{\equiv}CCO_2^- \rightarrow (RC{\equiv}C)_2 + 2CO_2 + 2e^- \quad (42)$$

$$[Co_xCl_y(R)_2]^- \rightarrow [Co_xCl_y]^- + (R)_2 \quad (43)$$

Along with uncovering the selectivity of C−H activation in silver alkynyl cations, $[RC{\equiv}CAg_2]^+$,[26d] we have discovered a 1,2-dyotropic rearrangement for dimethylcuprate (Figure 12).[27h] Initial isomerization to $[CH_3CH_2MH]^-$ (eq 44), with subsequent *β*-hydride elimination (eq 45), "reports" on this rearrangement reaction. Overall, the sequence corresponds to the metal promoted dehydro-decarboxylative coupling of two acetate ligands (eq 46).

$$[MeCuMe]^- \rightarrow [CH_3CH_2CuH]^- \quad (44)$$

$$[CH_3CH_2CuH]^- \rightarrow [HCuH]^- + CH_2{=}CH_2 \quad (45)$$

$$2MeCO_2^- \rightarrow CH_2{=}CH_2 + 2CO_2 + 2H^- \quad (46)$$

4.2. Photochemical Activation

Organometallic ions decompose differently under conditions of CID versus UV photodissociation.[26b,27n] $[MeAg_2]^+$ and $[PhAg_2]^+$ eliminate Ag^+ under CID (eq 47) but upon photolysis produce the new ionic products $[RAg]^{+\bullet}$ and $[Ag_2]^{+\bullet}$ via bond homolysis (eqs 48 and 49).[26b] Furthermore, comparisons between the theoretical and experimental UV−vis spectra (Figure 13) allow an unambiguous structural determination of $[PhAg_2]^+$, $[MeAg_2]^+$, and $[(Ph)_2Ag]^-$.[26b,27n]

$$[RAg_2]^+ \rightarrow Ag^+ + [RAg] \quad (47)$$

$$[RAg_2]^+ \rightarrow [RAg]^{+\bullet} + Ag^{\bullet} \quad (48)$$

$$[RAg_2]^+ \rightarrow [Ag_2]^{+\bullet} + R^{\bullet} \quad (49)$$

DOI: 10.1021/ar500377u
Acc. Chem. Res. 2015, 48, 329−340

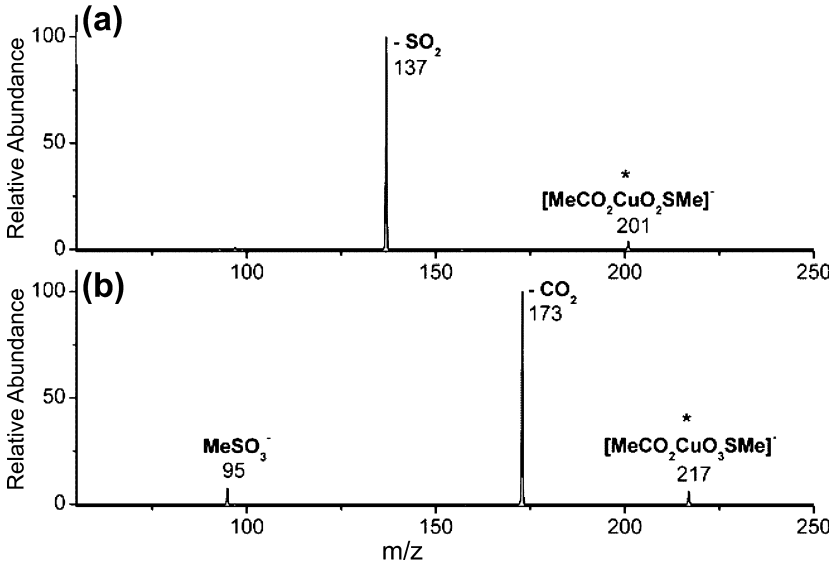

Figure 11. CID spectra of mass-selected (*) (a) $[MeCO_2Cu(O_2SMe)]^-$ and (b) $[MeCO_2Cu(O_3SMe)]^-$.

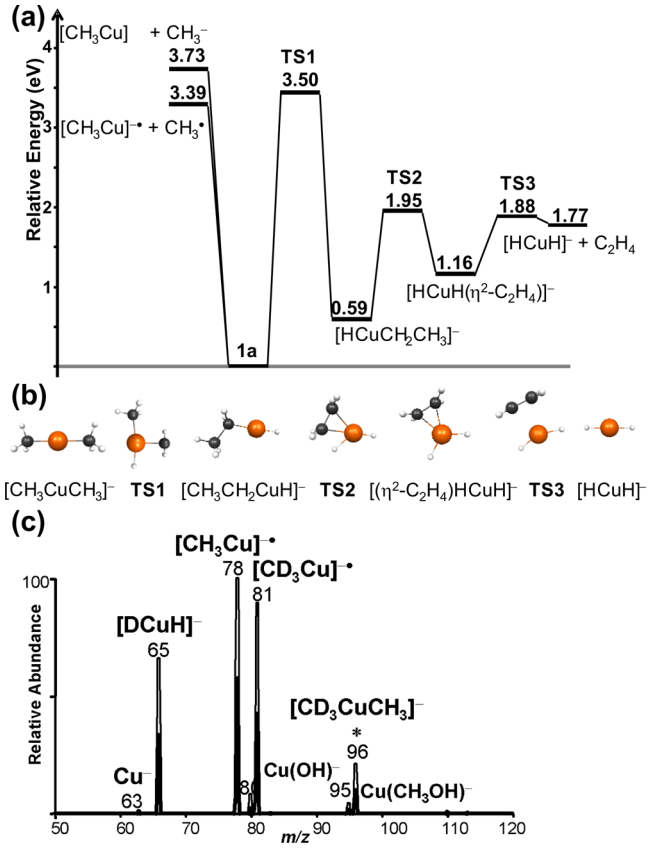

Figure 12. (a, b) DFT calculated potential energy diagram and key species associated with 1,2-dyotropic rearrangement and (c) CID of mass-selected (*) $[CD_3{}^{63}CuCH_3]^-$ showing selective formation of $[D^{63}CuH]^-$, *m/z* 66.

5. STOICHIOMETRIC AND CATALYTIC BIMOLECULAR REACTIONS OF ORGANOMETALLIC IONS

5.1. Reactions with Acids

5.1.1. Hydrolysis. Organometallic complexes can react with water via hydrolysis (eq 50), in some instances in competition with aquation (eq 51).

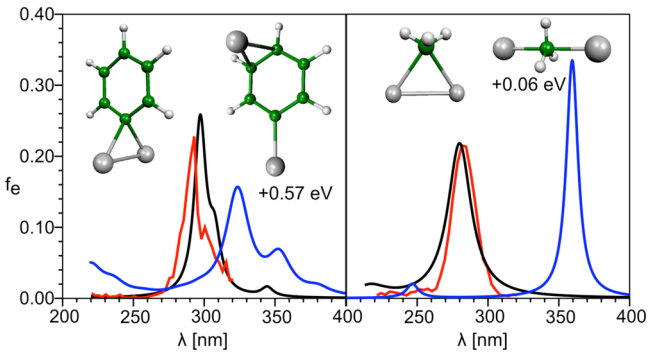

Figure 13. Comparison of calculated absorption spectra for the lowest energy isomer (black) and the second isomer (blue) of RAg_2^+ (R = Ph and Me) with the experimental photofragmentation spectrum (red). The structures of both isomers are given.

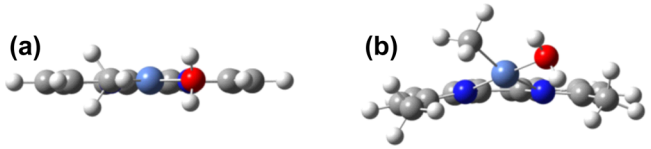

Figure 14. Deviation from planarity for the water adduct induced by the neocuproine auxiliary ligand: (a) planar $[MeNi(phen)(H_2O)]^+$ and (b) distorted $[MeNi(neo)(H_2O)]^+$.

$$[RM(L)_n]^x + H_2O \rightarrow [HOM(L)_n]^x + RH \quad (50)$$

$$[RM(L)_n]^x + H_2O \rightarrow [RM(L)_n(H_2O)]^x \quad (51)$$

The R and L group's basicity, sterics, and denticity tune this reactivity. In three-coordinate group 10 complexes, $[RM(phen))]^+$, hydrolysis (eq 50) occurs via a Lewis acid–base mechanism rather than oxidative addition/reductive elimination (OA/RE) and is more rapid for R = Me than for R = Ph[25a] and does not occur for R = $PhCH_2$, because η^3 binding hinders access by water. Steric crowding in the TS causes five-coordinate $[MeMg(O_2CMe)_2]^-$ to react more slowly than three-coordinate $[MeMg(Cl)_2]^-$ (eq 50),[27b] while the aquation the rates of $[RM(L)]^+$ (R = Me and Ph; M = Ni, Pd, and Pt) are slowed considerably when changing L = phen to bulkier neocuproine

DOI: 10.1021/ar500377u
Acc. Chem. Res. 2015, 48, 329–340

Scheme 3. Competing Mechanisms for Protodecarboxylation of the Organometallic $[MeM(phen)]^{+a}$

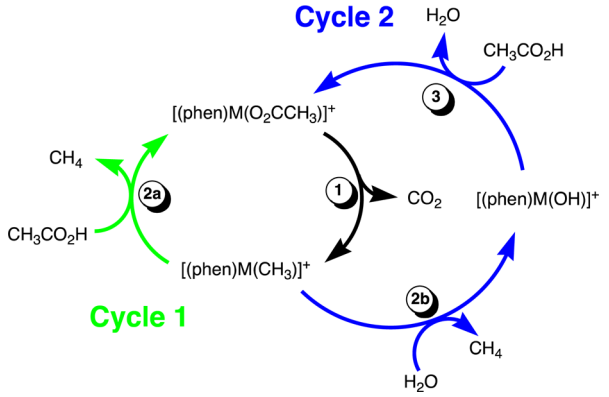

[a]Direct protodecarboxylation, step 2a; water catalyzed protodecarboxylation (hydrolysis, step 2b, then reaction with acetic acid, step 3).

(eq 51).[25a] The coordination complex reflects this (cf, Figure 14a,b); the neocuproine structure adopts a distorted square planar geometry.

The metal also tunes reactivity and selectivity. Comparing Li and Mg, experiment and RRKM theory reveal that $[HCCLi(Cl)]^-$ is more reactive than $[HCCMg(Cl)_2]^-$, the latter having higher entropic penalty for hydration.[27t] Just as a second metal center promotes decarboxylation, it enhances the reactivity toward water: the addition of LiCl to $[HCCLi(Cl)]^-$ or $[HCCMg(Cl)_2]^-$ by a factor of ~2 and the addition of $MgCl_2$ to $[HCCMg(Cl)_2]^-$ by a factor of ~4.[27t] For the group 10 $[RM(phen)]^+$ hydrolysis (eq 50) dominates when M = Ni, while for M = Pd and Pt aquation dominates (eq 51). This selectivity reflects the "hardness" of Ni^{2+} ion relative to Pt^{2+} and Pd^{2+} enhancing the aqua ligand's acidity.

5.1.2. Catalytic Protodecarboxylation. Catalytic protodecarboxylation of acetic acid yields CO_2 and CH_4 (eq 19). When catalyzed by group 10 $[MeM(phen)]^+$ cations, the reaction proceeds via two related cycles (Scheme 3).[25b] Decarboxylation of $[MeCO_2M(phen)]^+$ to form $[MeM(phen)]^+$ (step 1 of both cycles) follows the relative reactivity Pd > Pt > Ni. Direct reaction of $[MeM(phen)]^+$ with acetic acid regenerates the $[MeCO_2M(phen)]^+$ catalyst (cycle 1, step 2a). Alternatively, hydrolysis may form the hydroxide $[HOM(phen)]^+$ (cycle 2, step 2b), which reacts with acetic acid to reform the $[MeCO_2M(phen)]^+$ catalyst and water. Cycle 2 is only competitive for M = Ni, thereby being the most promising catalyst.[25b] Again, Lewis acid–base mechanisms are favored over OA/RE.

5.2. C–C Bond Coupling Reactions

5.2.1. Alkylation. The metal tunes reactivity in alkyations with methyl iodide. For example, due to a good HOMO/LUMO interaction, dimethylcuprate cross-couples via OA/RE (eq 52), while the Ag and Au congeners are unreactive.[27c,e,j]

$$[MeCuMe]^- + MeI \rightarrow [MeCuI]^- + CH_3CH_3 \quad (52)$$

Ligand effects on selectivity and reactivity were probed for $[MeCuR]^-$ (R = organyl or hydride ligands) by examining branching ratios (eqs 53 and 54) and kinetics, respectively.[27r]

$$[MeMR]^- + MeI \rightarrow [RMI]^- + CH_3CH_3 \quad (53)$$

$$[MeMR]^- + MeI \rightarrow [MeMI]^- + RCH_3 \quad (54)$$

All alkyl R groups exhibited similar reactivity, while bulkier, unsaturated groups resulted in lower reactivity. $[MeCuH]^-$ is 8

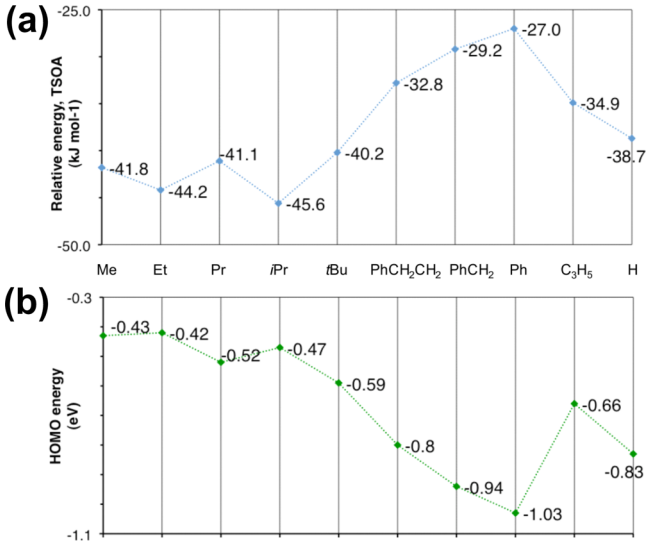

Figure 15. (a) Relative activation energy for oxidative addition of methyl iodide to $[MeCuR]^-$ (kJ mol^{-1}). (b) Highest occupied molecular orbital (HOMO) energies (eV) for $[MeCuR]^-$.

times more reactive than $[MeCuMe]^-$, demonstrating the intrinsic nucleophilicity of copper hydrides. Overall, while selectivity is controlled by RE, reactivity is kinetically controlled in the OA step. This energy is largely determined by the HOMO energy of the complex (Figure 15).

5.2.2. Allylation. Allylation is mechanistically complex, and in each case allyl intermediates played a key role in determining selectivity. For example, the reactions of $[MeMMe]^-$ (M = Cu, Ag, and Au) with allyl iodide proceeded via cross-coupling (eqs 55 and 56) in competition with homocoupling (eqs 57 and 58).[27k] $[MeCuMe]^-$ was found to be the most reactive but least selective due to the involvement of a kinetically unstable Cu(III) intermediate; $[MeAgMe]^-$ reacted less efficiently but resulted solely in nucleophilic substitution via direct reaction with the ligand, while $[MeAuMe]^-$ does not promote C–C bond coupling due to the stability of the Au(III) intermediate.[27k]

$$[MeMMe]^- + C_3H_5I \rightarrow [MeMI]^- + C_3H_5CH_3 \quad (55)$$

$$[MeMMe]^- + C_3H_5I \rightarrow I^- + [MeM] + C_3H_5CH_3 \quad (56)$$

$$[MeMMe]^- + C_3H_5I \rightarrow [C_3H_5MI]^- + CH_3CH_3 \quad (57)$$

$$[MeMMe]^- + C_3H_5I \rightarrow I^- + [C_3H_5M] + CH_3CH_3 \quad (58)$$

Products of reaction of the methyl palladalactone $[(Me)Pd(CH_2CO_2)]^-$ with allyl iodide are consistent with the formation of a key Pd(IV) intermediate, $[(Me)(I)(CH_2CHCH_2)Pd(CH_2CO_2)]^-$ (eq 59), which decomposes through allylation via RE (forming ions at m/z 291, $[(I)Pd(CH_2CO_2)]^-$, eq 60, or m/z 127, I^-, eq 61, Figure 16) or homocoupling via RE of propionate (eq 62).[27p] Another major side-reaction, iodide-atom abstraction, yields $[(Me)(I)Pd(CH_2CO_2)]^-$ (m/z 306, eq 63).

$$[(Me)Pd(CH_2CO_2)]^- + C_3H_5I \rightarrow [(Me)(I)(CH_2CHCH_2)Pd(CH_2CO_2)]^- \quad (59)$$

$$[(Me)(I)(CH_2CHCH_2)Pd(CH_2CO_2)]^- \rightarrow [(I)Pd(CH_2CO_2)]^- + C_3H_5CH_3 \quad (60)$$

DOI: 10.1021/ar500377u
Acc. Chem. Res. 2015, 48, 329–340

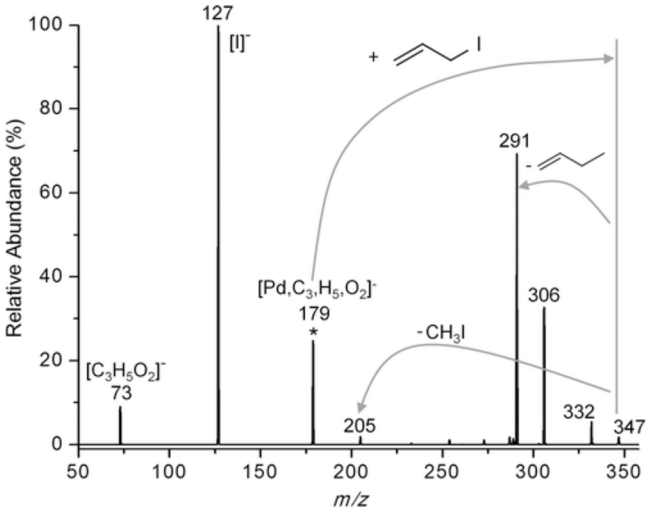

Figure 16. Ion−molecule reaction of mass-selected (*) $[(Me)Pd(CH_2CO_2)]^-$ with allyl iodide.

$$[(Me)(I)(CH_2CHCH_2)Pd(CH_2CO_2)]^- \rightarrow I^- + [Pd(CH_2CO_2)]^- + C_3H_5CH_3 \quad (61)$$

$$[(Me)(I)(CH_2CHCH_2)Pd(CH_2CO_2)]^- \rightarrow CH_3CH_2CO_2^- + [(I)PdC_3H_5] \quad (62)$$

$$[(Me)Pd(CH_2CO_2)]^- + C_3H_5I \rightarrow [(Me)(I)Pd(CH_2CO_2)]^- + CH_2CHCH_2^{\bullet} \quad (63)$$

Catalytic decarboxylative allylic-alkylation (eq 64) with the organometallic catalysts $[MeCuMe]^-$,[27e,o] $[MeM1M2]^+$ (M1 and M2 = Ag or Cu),[26e] and group 10 $[MeM(phen)]^+$ complexes[25c] has been reviewed.[30]

$$CH_3CO_2CH_2CHCH_2 \rightarrow CH_3CH_2CHCH_2 + CO_2 \quad (64)$$

6. CONCLUSIONS AND OUTLOOK

Metal-mediated decarboxylation has a rich history and is finding new applications alongside and in tandem with existing bond-transformation processes. Gas-phase studies provide a mechanistic basis for understanding decarboxylation processes in the condensed phase and present an opportunity to discover new reactions. By study of the decarboxylation process using ion trap mass spectrometers, the relative ease of decarboxylation can be systematically examined, the structures of resulting organometallic ions can be probed spectroscopically, and their fundamental unimolecular and bimolecular reactivity can be unveiled. Promising future directions include an examination of photocatalytic induced bond formation[31] and integrating gas-phase studies as a discovery tool[22b] for the "invention" of new condensed phase reactions.

AUTHOR INFORMATION

Corresponding Author

*Professor Richard O'Hair. Fax: +61 3 9347 5180. Tel: +61 3 8344 2452. E-mail: rohair@unimelb.edu.au.

Notes

The authors declare no competing financial interest.

Biographies

Richard A. J. O'Hair uses MS (i) to examine the fundamental chemistry of organic, inorganic, organometallic, and biological systems and (ii) in bioanalytical applications. Since his 2006 previously published biography,[23b] he has received the Morrison Medal, become an associate editor of the *Journal of the American Society for Mass Spectrometry*, joined the *Organometallics* Editorial Advisory Board, and been a visiting Professor at the Universités Pierre et Marie Curie (Paris) and Claude Bernard (Lyon).

Nicole J. Rijs received her Ph.D. (2012) from the University of Melbourne, exploring the decarboxylative formation and reactivity of organometallate anions. Currently, she is an Alexander von Humboldt fellow at the TU Berlin.

ACKNOWLEDGMENTS

R.A.J.O. thanks the ARC for support (Grant DP110103844 and the CoE program) and all the students, postdoctoral fellows, and collaborators involved in our decarboxylation work, especially Dr. George Khairallah. N.J.R. thanks the AvH Foundation.

REFERENCES

(1) Baudoin, O. New Approaches for Decarboxylative Biaryl Coupling. *Angew. Chem., Int. Ed.* **2007**, *46*, 1373−1375.
(2) (a) Hoyle, J. In *The Chemistry of Acid Derivatives*; Patai, S., Ed.; Wiley: Chichester, England, 1992; Chapter 11. (b) Taylor, R. In *The Chemistry of Acid Derivatives*; Patai, S., Ed.; Wiley: Chichester, England, 1992; Chapter 15.
(3) Deacon, G. B.; Faulks, S. J.; Pain, G. N. The Synthesis of Organometallics by Decarboxylation Reactions. *Adv. Organomet. Chem.* **1986**, *25*, 237.
(4) Huang, K.; Sun, C.-L.; Shi, Z.-J. Transition-Metal-Catalyzed C-C Bond Formation through the Fixation of Carbon Dioxide. *Chem. Soc. Rev.* **2011**, *40*, 2435−2452.
(5) Darensbourg, D. J.; Holtcamp, M. W.; Longridge, E. M.; Khandelwal, B.; Klausmeyer, K. K.; Reibenspies, J. H. Role of the Metal Center in the Homogeneous Catalytic Decarboxylation of Select Carboxylic Acids. Copper(I) and Zinc(II) Derivatives of Cyanoacetate. *J. Am. Chem. Soc.* **1995**, *117*, 318−328.
(6) Liu, A.; Zhang, H. Transition Metal-Catalyzed Nonoxidative Decarboxylation Reactions. *Biochemistry* **2006**, *45*, 10407−10411.
(7) Meyer, M. M.; Khairallah, G. N.; Kass, S. R.; O'Hair, R. A. J. Gas-Phase Synthesis and Reactivity of Lithium Acetate Enolate Anion, $^-CH_2CO_2Li$. *Angew. Chem., Int. Ed.* **2009**, *48*, 2934−2936.
(8) Pesci, L. Constituzione dei Composti Organo-Mercurici dell'Acido Benzoico. *Atti Accad. Naz. Lincei, Cl. Sci. Fis., Mat. Nat., Rend.* **1901**, *10* (v), 362−363.
(9) Whitmore, F. C.; Culhane, P. J. The Replacement of Carboxyl by Mercury in Certain 3-Substituted Phthalic Acids. *J. Am. Chem. Soc.* **1929**, *51*, 602−605.
(10) Kharasch, M. S. An Indirect Method of Preparation of Organic Mercury Derivatives and a Method of Linking Carbon to Carbon. *J. Am. Chem. Soc.* **1921**, *43*, 2238−2243.
(11) Shepard, A. F.; Winslow, N. R.; Johnson, J. R. The Simple Halogen Derivatives of Furan. *J. Am. Chem. Soc.* **1930**, *52*, 2083−2090.
(12) Hubacher, M. H. Determination of Carboxy Group in Aromatic Acids. *Anal. Chem.* **1949**, *21*, 945−947.
(13) Nilsson, M. A New Biaryl Synthesis Illustrating a Connection between the Ullmann Biaryl Synthesis and Copper-Catalyzed Decarboxylation. *Acta Chem. Scand.* **1966**, *20*, 423−426.
(14) (a) Weaver, J. D.; Recio, A.; Grenning, A. J.; Tunge, J. A. Transition Metal-Catalyzed Decarboxylative Allylation and Benzylation Reactions. *Chem. Rev.* **2011**, *111*, 1846−1913. (b) Rodriguez, N.; Goossen, L. Decarboxylative Coupling Reactions: A Modern Strategy for C-C-Bond Formation. *Chem. Soc. Rev.* **2011**, *40*, 5030−5048. (c) Shang, R.; Liu, L. Transition Metal-Catalyzed Decarboxylative Cross-Coupling Reactions. *Sci. China: Chem.* **2011**, *54*, 1670−1687. (d) Cornella, J.; Larrosa, I. Decarboxylative Carbon-Carbon Bond-Forming

DOI: 10.1021/ar500377u
Acc. Chem. Res. 2015, 48, 329−340

Transformations of (Hetero)aromatic Carboxylic Acids. *Synthesis* **2012**, 653−676. (e) Park, K.; Lee, S. Transition Metal-Catalyzed Decarboxylative Coupling Reactions of Alkynyl Carboxylic Acid. *RSC Adv.* **2013**, *3*, 14165−14182.
(15) Myers, A. G.; Tanaka, D.; Mannion, M. R. Development of a Decarboxylative Palladation Reaction and Its Use in a Heck-type Olefination of Arene Carboxylates. *J. Am. Chem. Soc.* **2002**, *124*, 11250−12251.
(16) Gooßen, L. J.; Deng, G.; Levy, L. M. Synthesis of Biaryls via Catalytic Decarboxylative Coupling. *Science* **2006**, *313*, 662−664.
(17) Shang, R.; Fu, Y.; Li, J.-B.; Zhang, S.-L.; Guo, Q.-X.; Liu, L. Synthesis of Aromatic Esters via Pd-Catalyzed Decarboxylative Coupling of Potassium Oxalate Monoesters with Aryl Bromides and Chlorides. *J. Am. Chem. Soc.* **2009**, *131*, 5738−5739.
(18) Rayabarapu, D. K.; Tunge, J. A. Catalytic Decarboxylative sp−sp^3 Coupling. *J. Am. Chem. Soc.* **2005**, *127*, 13510−13511.
(19) Tian, Z.; Kass, S. R. Carbanions in the Gas Phase. *Chem. Rev.* **2013**, *113*, 6986−7010.
(20) Reichert, C.; Fung, D. K. C.; Lin, D. C. K.; Westmore, J. B. Thermal Decomposition of Copper(II) Carboxylates: Mass Spectra of Binuclear Copper(I) Carboxylates. *Chem. Commun.* **1968**, 1094−1095.
(21) (a) Busch, K. L.; Cooks, R. G.; Walton, R. A.; Wood, K. V. Mass Spectrometric Investigation of Silver Ion Promoted Carbon-Carbon Bond Scission. *Inorg. Chem.* **1984**, *23*, 4093−4097. (b) Fiedler, A.; Schröder, D.; Zummack, W.; Schwarz, H. Reversible *β*-Hydrogen Transfer between $Fe(C_2H_5)^+$ and $HFe(C_2H_4)^+$: Case of Two-State Reactivity? *Inorg. Chim. Acta* **1997**, *259*, 227−235.
(22) (a) Henderson, W.; McIndoe, J. S. *Mass Spectrometry of Inorganic and Organometallic Compounds*; Wiley: Chichester, England, 2005. (b) Schröder, D. Applications of Electrospray Ionization Mass Spectrometry in Mechanistic Studies and Catalysis Research. *Acc. Chem. Res.* **2013**, *45*, 1521−1532.
(23) (a) O'Hair, R. A. J. Gas Phase Ligand Fragmentation to Unmask Reactive Metallic Species. In *MS Investigations of Reactive Intermediates in Solution*; Wiley-VCH: Weinheim, Germany, 2010; Chapter 6, pp 199−227. (b) O'Hair, R. A. J. The 3D Quadrupole Ion Trap Mass Spectrometer As a Complete Chemical Laboratory for Fundamental Gas-Phase Studies of Metal Mediated chemistry. *Chem. Commun.* **2006**, 1469−1481. (c) Gronert, S. Quadrupole Ion Trap Studies of Fundamental Organic Reactions. *Mass Specrom. Rev.* **2005**, *24*, 100−120. (d) McLuckey, S. A.; Goeringer, D. E. Slow Heating Methods in Tandem Mass Spectrometry. *J. Mass Spectrom.* **1997**, *32*, 461−474.
(24) (a) Gronert, S. Estimation of Effective Ion Temperatures in a Quadrupole Ion Trap. *J. Am. Soc. Mass Spectrom.* **1998**, *9*, 845−848. (b) Donald, W. A.; Khairallah, G. N.; O'Hair, R. A. J. The Effective Temperature of Ions Stored in a Linear Quadrupole Ion Trap Mass Spectrometer. *J. Am. Soc. Mass Spectrom.* **2013**, *24*, 811−815.
(25) (a) Woolley, M. J.; Khairallah, G. N.; da Silva, G.; Donnelly, P. S.; Yates, B. F.; O'Hair, R. A. J. Role of the Metal, Ligand and Alkyl Group in the Hydrolysis Reactions of Group 10 Organometallic Cations, $[(L)M(R)]^+$. *Organometallics* **2013**, *32*, 6931−6944. (b) Woolley, M. J.; Khairallah, G. N.; da Silva, G. R.; Donnelly, P. S.; O'Hair, R. A. J. Direct versus Water Mediated Protodecarboxylation of Acetic Acid Catalyzed by Group 10 Carboxylates, $[(phen)M(O_2CCH_3)]^+$. *Organometallics* **2014**, *33*, 5185−5197. (c) Woolley, M. J.; Ariafard, A.; Khairallah, G. N.; Donnelly, P. S.; Canty, A. J.; Yates, B. F.; O'Hair, R. A. J. Decarboxylative-Coupling of Allyl Acetate Catalysed by Group 10 Organometallics, $[(phen)M(CH_3)]^+$. *J. Org. Chem.* **2014**, *79*, 12056−12069.
(26) (a) Khairallah, G. N.; Waters, T.; O'Hair, R. A. J. C-C Bond Coupling Between the Organometallic Cations $CH_3Ag_2^+$, $CH_3Cu_2^+$ and CH_3AgCu^+ and Allyliodide. *Dalton Trans.* **2009**, 2832−2836. (b) Brunet, C.; Antoine, R.; Broyer, M.; Dugourd, P.; Kulesza, A.; Petersen, J.; Röhr, M. I. S.; Mitrić, R.; Bonačić-Koutecký, V.; O'Hair, R. A. J. Optical and Structural Properties of Organosilver Reactive Intermediates. *J. Phys. Chem. A* **2011**, *115*, 9120−9127. (c) Khairallah, G. N.; Williams, C. M.; Chow, S.; O'Hair, R. A. J. sp-sp^3 Coupling Reactions of Alkynylsilver Cations, $RC{\equiv}CAg_2^+$ (R = Me and Ph) with Allyliodide. *Dalton Trans.* **2013**, *42*, 9462−9467. (d) Khairallah, G. N.; Saleeba, K. A.; Chow, S.; Eger, W.; Williams, C. M.; O'Hair, R. A. J. C-H and C-C Bond Activation Reactions in Silver Alkynyl Cluster Cations, $RC{\equiv}CAg_2^+$. *Int. J. Mass Spectrom.* **2013**, *354*−*355*, 229−234. (e) Al Sharif, H.; Vikse, K. L.; Khairallah, G. N.; O'Hair, R. A. J. Catalytic Decarboxylative-Coupling of Allyl Acetate: Role of the Metal Centers in the Organometallic Cluster Cations $[CH_3Cu_2]^+$, $[CH_3AgCu]^+$ and $[CH_3Ag_2]^+$. *Organometallics* **2013**, *32*, 5416−5427.
(27) (a) O'Hair, R. A. J. Dimethylargenate Is a Stable Species in the Gas Phase. *Chem. Commun.* **2002**, 20−21. (b) O'Hair, R. A. J.; Vrkic, A. K.; James, P. F. Gas Phase Synthesis and Reactivity of the Organomagnesates $[CH_3MgL_2]^-$ (L = Cl and = O_2CCH_3): From Ligand Effects to Catalysis. *J. Am. Chem. Soc.* **2004**, *126*, 12173−12183. (c) James, P. F.; O'Hair, R. A. J. Dimethyl Cuprate Undergoes C−C Bond Coupling with Methyliodide in the Gas Phase but Dimethyl Argenate Does Not. *Org. Lett.* **2004**, *6*, 2761−2764. (d) Jacob, A. P.; James, P. F.; O'Hair, R. A. J. Do Alkali and Alkaline Earth Acetates Form Organometallates via Decarboxylation? A Survey Using Electrospray Ionization Tandem Mass Spectrometry And DFT Calculations. *Int. J. Mass Spectrom.* **2006**, *255*−*256*, 45−52. (e) Rijs, N.; Waters, T.; Khairallah, G. N.; O'Hair, R. A. J. Gas-Phase Synthesis of the Homo and Hetero Organocuprate Anions $[MeCuMe]^-$, $[EtCuEt]^-$, and $[MeCuR]^-$. *J. Am. Chem. Soc.* **2008**, *130*, 1069−1079. (f) Rijs, N.; O'Hair, R. A. J. Gas−Phase Synthesis of Organoargenate Anions and Comparisons with their Organocuprate Analogs. *Organometallics* **2009**, *28*, 2684−2692. (g) Khairallah, G. N.; Thum, C.; O'Hair, R. A. J. A Second Metal Center Enhances the Reactivity of an Organomagnesate: Comparison of the Gas Phase Reactions of Water with $RCCMgCl_2^-$ and $RCCMg_2Cl_4^-$ (R = H and Ph). *Organometallics* **2009**, *28*, 5002−5011. (h) Rijs, N. J.; Yates, B. F.; O'Hair, R. A. J. Dimethylcuprate Undergoes a Dyotropic Rearrangement. *Chem.—Eur. J.* **2010**, *16*, 2674−2678. (i) Rijs, N. J.; O'Hair, R. A. J. Unimolecular Reactions of Organocuprates and Organoargenates. *Organometallics* **2010**, *29*, 2282−2291. (j) Rijs, N. J.; Sanvido, G. B.; Khairallah, G. N.; O'Hair, R. A. J. Gas Phase Synthesis and Reactivity of Dimethylaurate. *Dalton Trans.* **2010**, *39*, 8655−8662. (k) Rijs, N. J.; Yoshikai, N.; Nakamura, E.; O'Hair, R. A. J. Gas-Phase Reactivity of Group 11 Dimethylmetallates with Allyl Iodide. *J. Am. Chem. Soc.* **2012**, *134*, 2569−2580. (l) Rijs, N. J.; O'Hair, R. A. J. Forming Trifluoromethylmetallates: Competition between Decarboxylation and C-F bond Activation of Group 11 Trifluoroacetate Complexes, $[CF_3CO_2ML]^-$. *Dalton Trans.* **2012**, *41*, 3395−3406. (m) Sraj, L. O.; Khairallah, G. N.; da Silva, G.; O'Hair, R. A. J. Who Wins: Pesci, Peters or Deacon? Intrinsic Reactivity Orders for Organocuprate Formation via Ligand Decomposition. *Organometallics* **2012**, *31*, 1801−1807. (n) Röhr, M. I. S.; Petersen, J.; Brunet, C.; Antoine, R.; Broyer, M.; Dugourd, P.; Bonačić-Koutecký, V.; O'Hair, R. A. J.; Mitrić, R. Synthesis and Spectroscopic Characterization of Diphenylargentate, $[(C_6H_5)_2Ag]^-$. *J. Phys. Chem. Lett.* **2012**, *3*, 1197−1201. (o) Rijs, N. J.; O'Hair, R. A. J. Dimethylcuprate-Catalyzed Decarboxylative Coupling of Allyl Acetate. *Organometallics* **2012**, *31*, 8012−8023. (p) Vikse, K. L.; Khairallah, G. N.; O'Hair, R. A. J. Gas-Phase Unimolecular Reactions of Pallada- and Nickela-lactones. *Organometallics* **2012**, *31*, 7467−7475. (q) Khairallah, G. N.; Thum, C. C. L.; Lesage, B.; Tabet, J.-C.; O'Hair, R. A. J. Gas-Phase Formation and Unimolecular Fragmentation Reactions of Organomagnesates, $[RMgX_2]^-$. *Organometallics* **2013**, *32*, 2319−2328. (r) Rijs, N. J.; Yoshikai, N.; Nakamura, E.; O'Hair, R. A. J. Unraveling Organocuprate Complexity: Fundamental Insights into Intrinsic Group Transfer Selectivity in Alkylation Reactions. *J. Org. Chem.* **2014**, *79*, 1320−1334. (s) Leeming, M.; Khairallah, G. N.; Osburn, S.; Vikse, K. L.; O'Hair, R. A. J. Cobalt-Mediated Decarboxylative Homocoupling of Alkynyl Carboxylic Acids. *Aust. J. Chem.* **2014**, *67*, 701−710. (t) Khairallah, G. N.; da Silva, G. R.; O'Hair, R. A. J. Molecular Salt Effects in the Gas Phase: Tuning the Kinetic Basicity of $[HCCLiCl]^-$ and $[HCCMgCl_2]^-$ by LiCl and $MgCl_2$. *Angew. Chem., Int. Ed.* **2014**, *53*, 10979−10983.
(28) Bachrach, S. M.; Hare, M.; Kass, S. R. Alkali Metal Salts of Dianions: A Theoretical and Experimental Study of $(C_6H_4)^{2-}M^+$ (M = Li and Na). *J. Am. Chem. Soc.* **1998**, *120*, 12646−12649.
(29) Vikse, K. L.; Khairallah, G. N.; McIndoe, J. S.; O'Hair, R. A. J. Fixed Charge Phosphine Ligands to Explore Coinage Metal-Mediated Decarboxylation Reactions. *Dalton Trans.* **2013**, *42*, 6440−6449.

DOI: 10.1021/ar500377u
Acc. Chem. Res. 2015, 48, 329−340

(30) O'Hair, R. A. J. Gas-Phase Studies of Metal Catalyzed Decarboxylative Cross-Coupling Reactions of Esters. *Pure. Appl. Chem.* **2014**, accepted for publication.
(31) Lang, S. B.; O'Nele, K. M.; Tunge, J. A. Decarboxylative Allylation of Amino Alkanoic Acids and Esters via Dual Catalysis. *J. Am. Chem. Soc.* **2014**, *136*, 13606−13609.

DOI: 10.1021/ar500377u
Acc. Chem. Res. 2015, 48, 329−340